

COMBINING SSM/I, TRMM AND INFRARED GEOSTATIONARY SATELLITE DATA IN A NEAR-REALTIME FASHION FOR RAPID PRECIPITATION UPDATES: ADVANTAGES AND LIMITATIONS

F. Joseph Turk¹, Jeff Hawkins¹, Eric A. Smith², Frank S. Marzano³, Alberto Mugnai⁴ and Vincenzo Levizzani⁵

¹Naval Research Laboratory, Marine Meteorology Division, 7 Grace Hopper Ave., Monterey, CA 93940 USA

²NASA Global Hydrology and Climate Center, 977 Explorer Blvd., Huntsville, AL 35806 USA

³University of L'Aquila, Dept. of Electrical Engineering, Monteluco di Roio, 67040 L'Aquila ITALY

⁴CNR-Institute of Atmospheric Physics, Area della Ricerca Tor Vergata, via Fosso del Cavaliere 100, 00133 Rome ITALY

⁵CNR-Institute of Atmospheric and Oceanic Sciences, via Gobetti 101, 40129 Bologna ITALY

ABSTRACT

We present an experimental technique to statistically blend low-Earth orbiting (LEO) passive microwave-based rainfall estimates from the Special Sensor Microwave Imager (SSM/I) and the Tropical Rainfall Measuring Mission (TRMM) microwave imagers together with geostationary-Earth orbiting (GEO) infrared satellite data in a near real-time, operationally-oriented fashion. The central idea involves utilizing the advantage of a geostationary-based measurement platform to capture the space-time evolution of precipitating clouds, and merging physically-based rain microphysical information available from LEO multi-frequency passive microwave measurements for a rapid-time update global precipitation analysis. The technique is designed to operate in an autonomous, operational mode and has potential usage in quantitative precipitation forecasting (QPF) and numerical weather prediction model applications. The 12-channel SEVERI instrument aboard the upcoming Meteosat Second Generation (MSG) geostationary satellite is well-suited for this type of combined technique. Examples will be shown from a global 0.25-degree precipitation analysis and also from a localized, intense rain event over central Italy.

1. Introduction.

A longstanding promise associated with meteorological satellite imaging systems has been accurate retrieval of precipitation on time and space scales consistent with the nature and development of precipitating clouds, i.e., a few hours and a few kilometers. Geostationary weather satellite imaging systems provide the rapid temporal update cycle needed to capture the growth and decay of precipitating cloud systems on a scale of several kilometers. At present, only the infrared (IR) region near 11 μm is suitable for diurnal sampling of the global precipitation process. As a result, IR sensors measure upwelling radiation that originates primarily near the tops of clouds, and any inferences to underlying precipitation are necessarily indirect (Arkin et. al, 1994). On the other hand, microwave-based imagers are better suited to quantitative measurement of precipitation due to the physical connection between upwelling microwave radiation and the underlying cloud precipitation structure. Owing to their longer wavelengths, the wider beamwidth of current real-aperture microwave imagers necessitates a low-Earth orbiting platform in order to achieve sufficient spatial resolution of clouds. The current Defense Meteorological Satellite Platform (DMSP) Special Sensor Microwave Imagers (SSM/I) are 7-channel passive microwave radiometric imagers in a near-polar orbit, with an on-Earth resolution of 15 km at 85.5 GHz. The SSM/I swath width of 1400 km does not assure contiguous coverage of the Earth between adjacent satellite orbits, and daily coverage from one satellite leaves coverage gaps in the tropics where the most of of the Earth's precipitation originates. The Tropical Rainfall Measuring Mission (TRMM) Microwave Imager

(TMI) improves upon the SSM/I heritage with the addition of a polarized 10.7 GHz channel, and improved spatial resolution by a factor of about 2.5 (Kummerow et. al, 1998). TRMM samples the tropics in a non-sun synchronous, low inclination orbit and the local sampling time progresses throughout the month.

Much of the current understanding of the strengths and weaknesses of passive microwave-based rainfall estimation were gained from the Algorithm Intercomparison Programs (AIP) coordinated by the Global Precipitation Climatology Project (GPCP). One of the important findings of AIP-3 (Ebert et al, 1998) was that for monthly rainfall products, the combined techniques performed better than the SSM/I-only techniques, whereas for instantaneous rain retrieval, the SSM/I-only techniques showed a better correlation with the validation data than did the combined algorithms (Smith et. al, 1998). The idea of blending LEO microwave and GEO infrared data together to introduce additional temporal sampling was proposed shortly after the launch of the first SSM/I and is an active area of research (Adler et. al, 1993, 1994; Vicente et. al, 1994, 1998; Levizzani et. al, 1996; Todd et. al, 1998; Xu et. al, 1999; Miller et. al, 2000). A major advantage of blending in the microwave-based data into the stream of geostationary data collection is the possibility of an hourly (or less) global rain rate analysis which avoids the spatial and temporal coverage gaps characteristic of swath-limited, low-Earth orbiting orbits. A complete rain analysis is needed for assimilation into numerical weather prediction (NWP) models, especially for quantitative precipitation forecasting, where models have traditionally had difficulties producing clouds and precipitation in the initial hours of the forecast period. Investigations of the impact of satellite-derived rain rates upon global and regional-scale numerical forecast models represents a growing body of literature. An important consideration of all of these investigations is a means to obtain rain rates at times and locations where SSM/I or TRMM data are not available. Techniques used include model physical initialization (Krishnamurti et. al, 1994; Rohaly and Van Tuyl, 1996), latent heat nudging (Jones and Macpherson, 1997), and more recent efforts have focused upon variational techniques (Marécal and Mahfouf, 1999). In general, these assimilation experiments have suggested that, currently, consistent information regarding the position of the precipitation affects forecast skill to a greater extent than errors in the quantitative amounts (Hou et. al, 1999).

We demonstrate examples from the geostationary-based technique to a regional-scale precipitation system in Europe, as well as an example of a global analysis from a blend of all five operational geostationary imagers. The central idea involves blending geostationary-based IR measurements to capture the space-time evolution of precipitating clouds with physically-based rain microphysical information available from LEO multi-frequency passive microwave measurements. We emphasize that a thorough ground-truth validation of this technique is ongoing but has not yet been completed. For a global technique such as this, a thorough validation involves coordinated comparisons with available radar and rain gauge data. Advantages and inherent limitations of this type of satellite-based precipitation analysis are discussed. Throughout the discussion, it is important to realize that we are working within the constraints of an operational forecast environment, where one is working with near real-time data and an imposed capability to accommodate dropped or missing periods of either type of satellite data.

2. Technique Description.

The quantification of rain rates from the geostationary IR data as implemented in a real-time fashion involves a autonomous process that is constantly co-locating, in space and time, newly arriving microwave and geostationary datasets. As of April 2000, there are four functional SSM/I imagers (F-11, 13, 14 and 15) and the single TMI, all with slightly different orbital crossing times. SSM/I or TMI data are examined immediately upon receipt for intersections in time and space with data from

any of the five current (April 2000) operational geostationary satellites (GOES-8 and 10, GMS-5, and Meteosat-5 and 7). Figure 1 shows a block diagram of the overall processing flow. When a given image pixel from a SSM/I (TMI) overpass occurs within 15 minutes of a GEO pixel, the spatially-coincident geostationary IR data are extracted, averaged and map-registered onto the SSM/I (TMI) sensor scan coordinate system. The SSM/I rain rate is computed via the operational NOAA-NESDIS scheme (Ferraro, 1997), which is computed at the A-scan sampling spacing (25 km) of the SSM/I scan grid. For TMI data, the real-time level 2A12 instantaneous rain rates are used directly (Kummerow et. al, 1998) and are provided on the 85 GHz scan grid of the TMI, where samples are spaced ≈ 7 -km along track and 4-km across-track. Files are saved with the co-located SSM/I or TMI rain rate, the IR temperatures, and the pixel geolocation. This process continues autonomously, immediately upon receipt of newly captured SSM/I and TMI datasets.

The presence of distinctly evolving rain systems is accommodated by subdividing the Earth into 15-degree boxes between ± 60 degrees latitude, spaced every 5-degrees apart (15-degrees encompasses the approximate swath width of the SSM/I instrument). This provides a spatial overlap to assure that the statistical relationships transition smoothly from adjacent regions. Once every hour, a cron-based update cycle starts and processes the aforementioned statistics files in time from newest-to-oldest, using the geolocation data to gradually construct separate histograms of the IR temperatures and the associated rain rate in each 15-degree box. To utilize only the most recent rain evolutionary history, these two histograms are accumulated until the percent coverage of a given box exceeds a 75-percent coverage threshold (the larger the percent threshold, the longer one needs to look back in time, which in turn draws upon an increasingly earlier stage of the cloud lifecycle).

To illustrate, Figure 1 depicts a single 15-degree box, which is further discretized into an inner grid with a spacing of 0.25 degrees. In this example, the first (most recent in time) SSM/I pass covers nearly all of the box. An earlier TMI pass (the narrower swath) adds additional points to the histogram accumulations, overlapping with the SSM/I and also increasing the total percent coverage.

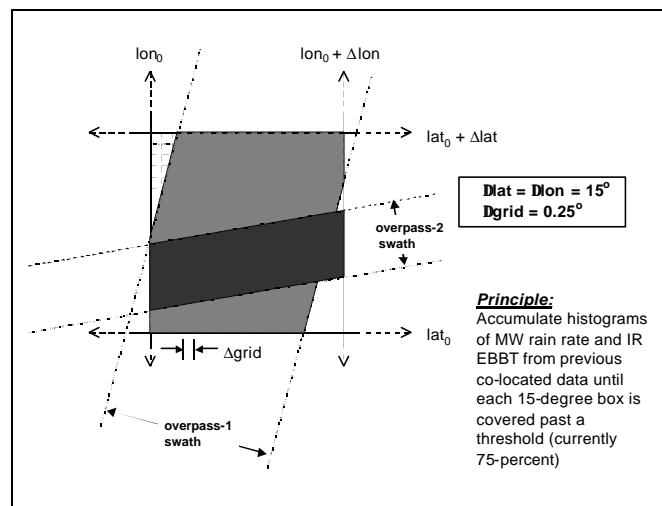


Figure 1. Depiction of an individual 15-degree region and how successively older (with respect to real time) LEO microwave-based satellite data overpasses are used to calculate a percent-coverage. Overpass 1 depicts an SSM/I swath; orbit 2 a narrower swath from the TMI.

This process continues with increasingly older-in-time statistics files until the box percent-coverage exceeds the percent threshold. Depending upon how recently a given geographical region was imaged by an SSM/I or TMI, the overall data used in some of the histogram boxes may be only a few hours old, whereas other regions may require more look-back time to reach the coverage threshold.

Currently, we set a maximum look-back time limit of 24 hours on the process. If a region has not reached the coverage threshold by this time, the histograms for this region are marked bad, and (temporarily) a geostationary-based rain estimate is unavailable for this region. However, eventually an update cycle will capture newly-arrived microwave data that have arrived in this region. We stress that these thresholds have not been examined in detail. Looking back past the previous 24 hours or more than 75-percent coverage runs the risk of tuning the IR brightness temperatures and the microwave-based rain rates with too much information from an earlier stage of the precipitation lifecycle. The sun-synchronous orbit inclination of the SSM/I provides more coverage at latitudes above 40 degrees than it does near the equator, whereas the TRMM orbit inclination fills in the SSM/I coverage gaps in the equatorial regions at different local times each day.

For the case of satellite data, the probability matching method (PMM; Crosson et. al, 1996) relates the probability distribution functions (PDF) of the microwave-based rain rate $P(R)$ and the geostationary IR brightness temperatures $P(T_B)$, respectively. The rain rate PDF $P(R)$ is matched while accumulating $P(T_B)$ from the warm end in brightness temperature on upwards and producing a series of matched $(T_{B,i}, R_i)$ pairs. The $(T_{B,0}, R_0)$ pair is the first pair to be matched; that is, zero-rain rate IR T_B threshold. After processing the past statistics as described, the hourly update cycle writes out a file that contains the lookup table for each 15-degree box, which relates the IR temperature to the microwave-based rain rate.

This type of procedure inherently allows tracking of a cloud pixel evolutionary lifecycle, but with a latency time, which depends upon the most recent receipt of microwave-based data. The latency time could be anywhere from an hour to up to 24-hours, depending upon the local crossing time of the LEO satellite patterns. Also, the zero-rain rate IR temperature threshold is adjusted automatically as the first step in the histogram matching, when the zero-rain rate points are matched.

When a new geostationary pass arrives and is post-processed, the calculation of instantaneous rain rates involves a straightforward scan of the above-mentioned global lookup tables that relates IR brightness temperatures to the histogram-matched microwave-based rain rates. This makes the calculation of per-pixel rain rate computationally rapid. Each pixel in the input geostationary data is assigned the nearest 15-degree histogram box. The pixel is then assigned a rain rate from an inverse-distance weighted average of this box's rain rate lookup table and the eight other boxes surrounding it. This type of compositing maintains a smooth transition in rain rate from pixel-to-pixel throughout the image. Multi-hour rain accumulations are computed by an explicit time-integration of successive instantaneous rain rate images. To address the effect of high, non-raining clouds such as cirrus clouds, the previous time history of the IR data is examined following the technique proposed and implemented by Vicente et. al (1998). If the IR temperature has significantly increased since the previous-time image (within the past hour), then the cloud is assumed to be in a decaying stage and the rain rate is adjusted based on the IR temperature difference. We are currently implementing tests for orographically-produced rain using NWP model data. This is a critical factor which is necessary whenever IR data are used to track precipitating clouds across high elevation terrain.

3. A Global 0.25-Degree Rainfall Analysis.

A global rainfall analysis is generated from this technique by accumulating instantaneous rain rate products as they are computed from the update cycle of each of the geostationary-based satellite imagers. Each IR data are projected onto a rectangular 0.25-degree map projection after they are averaged to this same resolution (data more than 50-degrees away from the satellite subpoint is omitted). From this, the nearest-time lookup tables produced by the histogram-matching procedure

are consulted and the instantaneous rain rate field is produced. At each 3-hourly synoptic time (0, 3,...21 UTC), accumulations are produced by time-integrating over the previous-time files. The length of the time accumulations is limited only by the amount of files maintained online; routinely we produce up to 168-hour (1-week) accumulation updates each 6 hours.

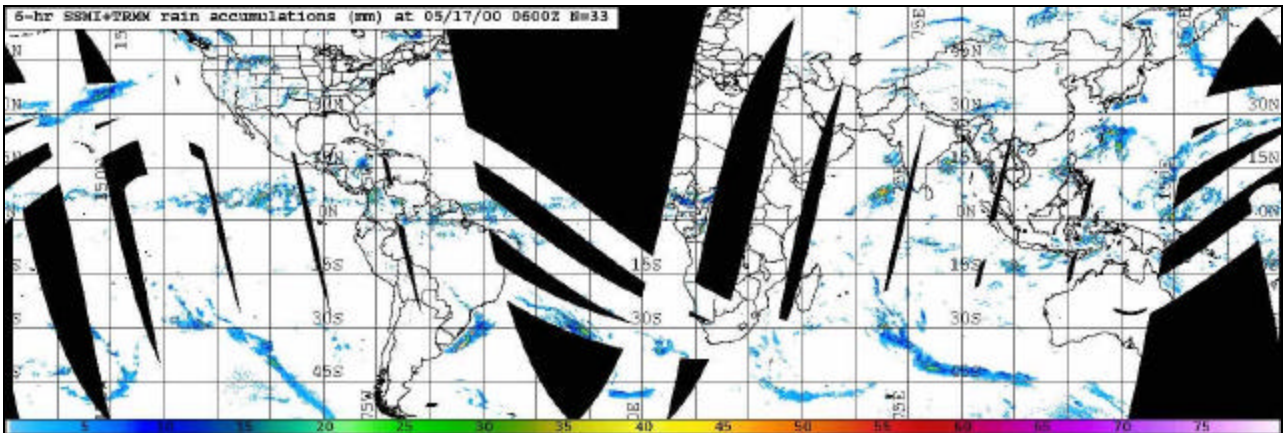


Figure 2. Previous 6-hour rain accumulations (in millimeters) valid at 0600 UTC on 17 May 2000 on a 0.25-degree rectangular map projection, from an average of all SSM/I (F-11,13,14 ,15) and TMI passes (33 overpasses total).

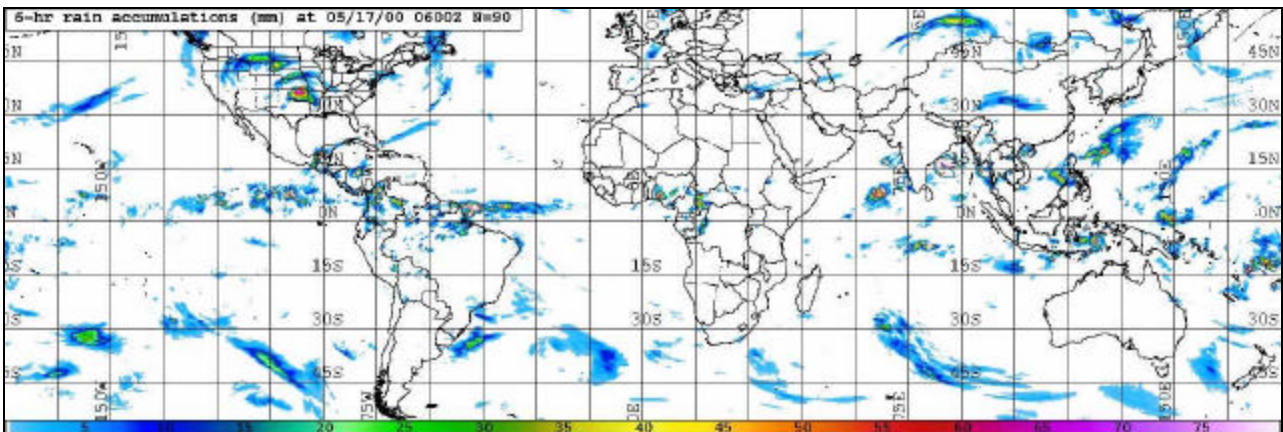


Figure 3. Same as Figure 2, except that the accumulations were obtained by the geostationary-based rain technique (in this example, an explicit time integration of instantaneous rain rate from 90 total images from GOES-8/10, Meteosat-5/7, GMS-5).

Figure 2 depicts the 6-hour microwave-only rain accumulations at 0600 UTC on 17 May 2000. The narrow swaths in the tropical band show the narrower swath of the TMI instrument versus those from the SSM/I. Figure 3 shows the rain accumulation over the same interval, from the geostationary-based technique, using a total of 90 instantaneous rain files from all five geostationary imagers. In general, there is strong agreement in the main precipitation features, although the geostationary technique has a tendency to assign light rain to areas surrounding the precipitation cores. Outside of the complete spatial coverage of Figure 4, several features are also captured: a strong outbreak of land-based precipitation in the southern Great Plains of the United States, and an improved definition of tropical activity in the southwest Pacific Ocean. While we have not yet validated the geostationary-based technique (especially important at these short time intervals), the need for a

spatially complete rain analysis implies the use of blended geostationary IR and microwave-based techniques such as this.

Turk et. al. (2000) examined the impact of the geostationary-based rain rates upon on the forecast skill of the Naval Operational Global Analysis and Prediction System (NOGAPS) in a tropical environment via a physical initialization technique. The forecast model impact was examined during an eight day period (21 –29 September 1998) from the Atlantic hurricane season. The 24, 36 and 48-hour physically initialized forecasts for Hurricane Georges showed positive impacts to hurricane positioning ranging from 12 to 16 percent, although the improvement fell to nearly no-impact at 72-hours for this particular storm. Typically, a 10-15 percent improvement in the location of the central minimum pressure after 24 hours were observed with a retention of this skill improvement out to 48 hours. While a single case study is not a measure of success or failure, impact scores of this level are promising and suggest the need for this type of improved rainfall analysis on a rapid-update (3-hours or less) time scale.

3. Examples from Localized Rainfall Over Central Italy.

Since the geostationary-based technique takes advantage of localized microwave-based rain rates, it is worthwhile to examine the characteristics of the geostationary-based rain accumulations in a smaller, localized regime, where depiction of finer-scale, rapidly evolving precipitation events may be missed due to infrequent microwave imager overpasses. During the afternoon of May 15, heavy rains and several mudslides were reported in south-central Italy. Figure 4 compares a 24-hour rainrate accumulation over Italy and the Mediterranean Sea at 0300 UTC on 16 May 2000.

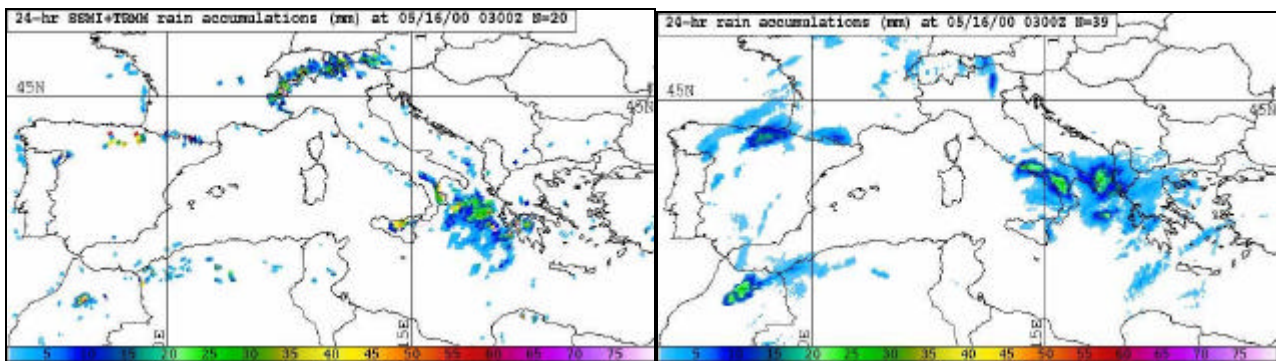


Figure 4. Left: Previous 24-hour rain accumulations (in millimeters) valid at 0300 UTC on 16 May 2000 over Italy and the Mediterranean Sea, from an average of all SSM/I (F-11,13,14 ,15) and TMI passes (20 overpasses total). Right: accumulations obtained by the geostationary-based rain technique (in this example, an explicit time integration of instantaneous rain rate from 39 consecutive Meteosat-7 images).

The microwave-only image (left image) is based on a composite average of the previous 24-hours of overpasses from all SSM/I and TMI passes (TMI extends only to 38 N latitude), whereas the geostationary-based (Meteosat-7) rain accumulation was generated via an explicit time integration of the 39 images during this time interval. Although the SSMI+TMI composite depicts coverage over all of Italy, the overpasses occurred at a time when the SSM/I rainfall algorithm detected precipitation over the Gulf of Taranto and the southern regions of Calabria and Sicily. Some false identification of precipitation is evident in the Alps. However, the half-hourly time sampling capabilities of the geostationary-based technique captured the rain events that occurred south of Rome along the Mediterranean coast and also in the narrow region between Italy and Albania (green

colors). While the problem of the light rain surrounding the cores is obvious, the regions of intense rain are well-captured and easily depicted on an animation.

5. Conclusions.

We have demonstrated a near-real time, operationally-oriented technique for blending geostationary infrared and low Earth-orbiting microwave-based satellite data for a rapid-update global rainfall analysis. The technique takes advantage of the complementary properties of geostationary and low-Earth orbiting sensors; namely, the inherent physical connection between passive microwave-based rain rate estimates and the finer scale, rapid time infrared-based update available from geostationary orbiting imagers. While we have not yet presented a thorough validation test, the technique has demonstrated the capability to produce a global rain rate analysis that is consistent with time- and space-coincident rain rate retrievals taken from the SSM/I and TMI microwave imagers. We are currently further investigating the impact of this rain analysis in a superensemble forecast, and are in the process of a validation phase with an extensive ground-based rain gauge network. Experimental imagery and results can be viewed online through the NRL Monterey website at <http://kauai.nrlmry.navy.mil/sat-bin/rain.cgi>.

Acknowledgements. The first two authors gratefully acknowledge support from the Office of Naval Research, Program Element (PE-060243N), and the Space and Naval Warfare Systems Command, PMW-185 (PE-0603207N). The last three authors wish to acknowledge the Consiglio Nazionale delle Ricerche (CNR) for support under Progetto Strategico MAP-SOP and Gruppo Nazionale per la Difesa dalle Catastrofi Idrogeologiche. Agenzia Spaziale Italiana (ASI) provided the contract *Studio del Ciclo Idrologico da Piattaforme Satellitari: Nube e Precipitazioni*.

REFERENCES

- Adler, R.F., A.J. Negri, P.R. Keehn, I.A. Hakkarinen, 1993: Estimation of monthly rainfall over Japan and surrounding waters from a combination of low-orbit microwave and geosynchronous IR data. *J. Appl. Meteor.*, **32**, 335-356.
- Adler, R.F., G.J. Huffman, and P.R. Keehn, 1994: Global tropical rain estimates from microwave-adjusted geosynchronous infrared data. *Remote Sens. Rev.*, **11**, 125-152.
- Arkin, P.A., R. Joyce, J.E. Janowiak, 1994: The estimation of global monthly mean rainfall using infrared satellite data: The GOES Precipitation Index (GPI). *Rem. Sens. Rev.*, **11**, 107-124.
- Crosson, W.L., C.E. Duchon, R. Raghavan, S.J. Goodman, 1996: Assessment of rainfall estimates using a standard Z-R relationship and the probability matching method applied to composite radar data in central Florida. *J. Appl. Met.*, **35**, 1203-1219.
- Ebert, E.E., and M.J. Manton, 1998: Performance of satellite rainfall estimation algorithms during TOGA-COARE, *J. Atmos. Science*, **55**, 1537-1557.
- Ferraro, R.R., 1997: Special sensor microwave imager derived global rainfall estimates for climatological applications. *J. Geophys. Res.*, **102**, D14, 16715-16735.
- Hou, A.Y., D.V. Ledvina, A.M. da Silva, S.Q. Zhang, J. Joiner, R. M. Atlas, 1999: Assimilation of SSM/I-derived surface rainfall and total precipitable water for improving the GEOS analysis for climate studies. *Month. Weath. Rev.*, submitted.

- Jones, C.D. and B. Macpherson, 1997: A latent heat nudging scheme for the assimilation of precipitation data into an operational mesoscale model. *Meteor. Appl.*, **4**, 269-277.
- Krishnamurti, T.N., G. Rohaly and H.S. Bedi, 1994: On the improvement of precipitation forecast skill from physical initialization. *Tellus*, **46A**, 598-614.
- Kummerow, C., W. Barnes, T. Kozu, J. Shiue, J. Simpson, 1998: The Tropical Rainfall Measuring Mission (TRMM) sensor package. *J. Atmos. Ocean. Tech.*, **15**, 809-817.
- Levizzani, V., F. Porcu, F.S. Marzano, A. Mugnai, E.A. Smith and F. Prodi, 1996: Investigating a SSM/I microwave algorithm to calibrate Meteosat infrared instantaneous rain rate estimates. *Meteo. Appl.*, **3**, 5-17.
- Marécal, V., and J.F. Mahfouf, 1999: Variational retrieval of temperature and humidity profiles from TRMM precipitation data. *Month. Weath. Rev.*, in press.
- Miller, S.W., P.A. Arkin, R. Joyce, 2000: A combined microwave/infrared rain rate algorithm. *J. Rem. Sens.*, accepted and in press.
- Rohaly, G., and A.H. Van Tuyl, 1996: Impact of physical initialization on the Navy Operational Global Atmospheric Prediction System (NOGAPS). *11th AMS Conf. Numerical Weath. Pred.*, 19-23 August, Norfolk, VA, USA, 287-289.
- Smith, E.A., and others, 1998: Results of the WetNet PIP-2 Project. *J. Appl. Meteor.*, **55**, 1483-1536.
- Todd, M.C., E.C. Barrett, M.J. Beaumont, and T.J. Bellerby, 1998: Estimation of daily rainfall over the upper Nile river basin using a continuously calibrated satellite infrared technique. *Meteor. Appl.*, **5**, 1-10.
- Turk, F.J., G. Rohaly, J.D. Hawkins, E.A. Smith, A. Grose, F.S. Marzano, A. Mugnai and V. Levizzani, 2000: Analysis and assimilation of rainfall from blended SSM/I, TRMM and geostationary satellite data, *10th Conf. On Satellite Meteorology and Oceanography*, AMS, Long Beach, CA., 66-69.
- Vicente, G.A., 1994: Hourly retrieval of precipitation rate from the combination of passive microwave and infrared satellite measurements. Ph.D. dissertation, Univ. of Wisconsin, Madison, WI, USA.
- Vincente, G.A., R.A. Scofield, W.P. Menzel, 1998: The Operational GOES Infrared Rainfall Estimation Technique. *Bull. Amer. Meteor. Soc.*, **79**, 1883-1898.
- Xu, L., X. Gao, S. Sorooshian, P.A. Arkin, B. Imam., 1999: A microwave infrared threshold technique to improve the GOES Precipitation Index. *J. Appl. Meteor.*, **38**, 569-579.